



Published in final edited form as:

Cell Metab. 2013 December 3; 18(6): . doi:10.1016/j.cmet.2013.10.011.

Activation of Calcium/Calmodulin-Dependent Protein Kinase II in Obesity Mediates Suppression of Hepatic Insulin Signaling

Lale Ozcan^{1,*}, Jane Cristina de Souza¹, Alp Avi Harari¹, Johannes Backs⁴, Eric N. Olson⁵, and Ira Tabas^{1,2,3,*}

¹Department of Medicine, Columbia University, New York, NY 10032, USA

²Department of Physiology and Cellular Biophysics, Columbia University, New York, NY 10032, USA

³Department of Pathology and Cell Biology, Columbia University, New York, NY 10032, USA

⁴Laboratory for Cardiac Epigenetics, Department of Cardiology, Heidelberg University, and DZHK-German Centre for Cardiovascular Research, Heidelberg 69120, Germany

⁵Department of Molecular Biology, University of Texas Southwestern Medical Center, Dallas, Texas 75390, USA

SUMMARY

A hallmark of obesity is selective suppression of hepatic insulin signaling (“insulin resistance”), but critical gaps remain in our understanding of the molecular mechanisms. We now report a major role for hepatic CaMKII, a calcium-responsive kinase that is activated in obesity. Genetic targeting of hepatic CaMKII, its downstream mediator p38, or the p38 substrate and stabilizer MK2 enhances insulin-induced p-Akt in palmitate-treated hepatocytes and obese mouse liver, leading to metabolic improvement. The mechanism of improvement begins with induction of ATF6 and the ATF6 target p58^{IPK}, a chaperone that suppresses the PERK—p-eIF2 α —ATF4 branch of the UPR. The result is a decrease in the ATF target TRB3, an inhibitor of insulin-induced p-Akt, leading to enhanced activation of Akt and its downstream metabolic mediators. These findings increase our understanding of the molecular mechanisms linking obesity to selective insulin resistance and suggest new therapeutic targets for type 2 diabetes and metabolic syndrome.

INTRODUCTION

Obesity is the leading cause of insulin resistance, metabolic syndrome, and type 2 diabetes (T2D), but therapeutic options are limited due to critical gaps in our knowledge of molecular mechanisms linking obesity with the metabolic disturbances of insulin resistance and T2D (Samuel and Shulman, 2012). A key factor in T2D is an inappropriate increase in hepatic glucose production (HGP), which results from selective hepatic insulin resistance together with impaired suppression of glucagon signaling (Lin and Accili, 2011). In addition to

© 2013 Elsevier Inc. All rights reserved.

*Correspondence: iat1@columbia.edu (I.T.) or lo2192@columbia.edu (L.O.).

SUPPLEMENTAL INFORMATION

Supplemental Information includes six figures and Supplemental Experimental Procedures.

Publisher's Disclaimer: This is a PDF file of an unedited manuscript that has been accepted for publication. As a service to our customers we are providing this early version of the manuscript. The manuscript will undergo copyediting, typesetting, and review of the resulting proof before it is published in its final citable form. Please note that during the production process errors may be discovered which could affect the content, and all legal disclaimers that apply to the journal pertain.

elevated HGP, selective insulin resistance contributes to other critical maladies associated with T2D, including cardiovascular disease, the leading cause of death in these patients (Bornfeldt and Tabas, 2011; Leavens and Birnbaum, 2011).

We recently elucidated a new pathway through which glucagon stimulates HGP and in fasting and in obesity, and in obesity this pathway contributes to hyperglycemia (Ozcan et al., 2012; Wang et al., 2012). The pathway is triggered downstream of the glucagon receptor by PKA-mediated activation of the endoplasmic reticulum (ER) calcium release channel, inositol 1,4,5-trisphosphate receptor (IP3R). Channel opening, which is also promoted by a glucagon receptor-phospholipase C pathway that generates IP3, results in release of calcium from ER stores, which then activates the cytoplasmic calcium-sensitive kinase, calcium/calmodulin dependent-protein kinase II (CaMKII). CaMKII then activates the MAPK p38 α , which phosphorylates FoxO1 in a manner that promotes FoxO1 nuclear translocation. Nuclear FoxO1 induces target genes that are rate-limiting for glycogenolysis and gluconeogenesis, notably, *G6pc* and *Pck1*. This CaMKII-FoxO1 pathway is complemented by the activation of the calcium-sensitive phosphatase calcineurin, which promotes CRTC2-mediated induction of the FoxO1 transcriptional partner, PGC1 α (Wang et al., 2012). Moreover, recent studies have shown that calcium transport back into the ER, mediated by sarcoplasmic/endoplasmic reticulum calcium ATPase (SERCA), is dysfunctional in obesity (Fu et al., 2011; Park et al., 2010), which could contribute to both the amplitude and duration of the pathological calcium response. Collectively, these data point to the importance of intracellular calcium metabolism and CaMKII in enhanced HGP in obesity. However, a critical remaining question in this area was whether CaMKII plays a role in the other major pathological process in obesity and T2D, namely, selective insulin resistance.

Defective insulin signaling is a major feature of selective hepatic insulin resistance in obesity (Brown and Goldstein, 2008; Konner and Bruning, 2012). In normal physiology, insulin stimulates insulin autophosphorylation of the insulin receptor (IR), which promotes to Tyr-phosphorylation of insulin receptor substrates 1 and 2 (IRS-1/2). Through a series of downstream processes involving lipid mediators and protein kinases, p-IRS-1/2 leads to Ser/Thr-phosphorylation and activation of Akt (also known as protein kinase B) (Saltiel and Kahn, 2001). Akt-induced phosphorylation of a number of substrates is critically involved in promoting the anabolic effects of insulin on glucose and lipid metabolism. In obesity and T2D, insulin-induced phosphorylation of Akt is defective, which disables the pathway that normally suppresses HGP (Lin and Accili, 2011). In theory, defective Akt phosphorylation could occur at the level of the insulin receptor, IRS1/2, signal transducers downstream of IRS-1/2, or Akt phosphorylation itself. Studies in obese mouse models have shown evidence for defects in each of these steps, depending on the model used and the focus of the investigation, and there is also evidence for defects in insulin-induced p-Akt in humans with T2D (Brozinick et al., 2003; Krook et al., 1998; Saad et al., 1992). Moreover, the resulting hyperinsulinemia excessively stimulates non-resistant insulin pathways that mediate hepatic lipid synthesis and storage (Brown and Goldstein, 2008) and is associated with other maladies associated with T2D, such as atherosclerosis (Bornfeldt and Tabas, 2011; Leavens and Birnbaum, 2011). Because perturbation of proximal insulin signaling is one of the earliest hallmarks of T2D and is responsible for the most important complications of obesity and T2D, identification of the molecular mechanisms responsible for this defect has the potential to aid in the development of new and more specific anti-diabetic drugs.

In this report, we identify a CaMKII/p38-mediated pathway that plays a critical role in obesity-associated insulin resistance in the liver. This pathway is independent of the aforementioned CaMKII/p38-FoxO1 pathway involved in HGP in obesity. We provide evidence that obesity-activated CaMKII/p38 suppresses insulin-induced Akt phosphorylation by activating the ER stress effector ATF4, which in turn induces the Akt

inhibitor, TRB3. Thus, an integrated, calcium-based paradigm in hepatocytes involved in the two cardinal features of T2D, hyperglycemia and defective insulin signaling, is beginning to emerge, providing new potential therapeutic targets.

RESULTS

Inhibition of Liver CaMKII, p38 α , or MAPKAPK2 (MK2) in Obese Mice Lowers Plasma Insulin and Improves the Response to Glucose Challenge

We first evaluated the role of CaMKII on plasma insulin levels and response to glucose in three models of obese mice. In the first model, liver CaMKII in *ob/ob* mice was inhibited through the use of an adenoviral vector expressing K43A-CaMKII (Pfleiderer et al., 2004), which is a kinase-inactive, dominant-negative form that has been shown to inhibit hepatic CaMKII (Ozcan et al., 2012). We showed previously that adeno-K43A-CaMKII treatment of *ob/ob* mice, as compared with *ob/ob* mice treated with adeno-LacZ control vector, lowered blood glucose (Ozcan et al., 2012). This effect occurred in the absence of any change in body weight (44.8 ± 1.9 vs. 43.5 ± 1.6 g), food intake (5.3 ± 0.3 vs. 5 ± 0.2 g per mouse per day), or epididymal fat pad mass (3.2 ± 0.2 vs. 3 ± 0.1 g). Moreover, K43A-CaMKII-treated mice displayed a more than twofold reduction in plasma insulin concentration compared with control adeno-LacZ-treated mice (Figure 1A), consistent with an increase in insulin sensitivity. In support of this conclusion, adeno-K43A-CaMKII treated *ob/ob* mice exhibited significantly lower glucose levels during glucose and insulin tolerance tests (Figure 1B–C).

In the second model, liver CaMKII γ , which is the CaMKII isoform in hepatocytes, was deleted in diet-induced obese (DIO) mice by injecting DIO *Camk2g^{fl/fl}* mice with adeno-associated virus-8 encoding Cre recombinase driven by the hepatocyte-specific thyroxine-binding globulin promoter (AAV8-TBG-Cre) (Sun et al., 2012). This treatment successfully silenced *Camk2g* in the hepatocytes (Figure 1D) without changing body weight (44.6 ± 2.29 vs. 43 ± 0.7 g), food intake (3.13 ± 0.17 vs. 2.92 ± 0.19 g per mouse per day), or epididymal fat pad mass (2.4 ± 0.14 vs. 2.24 ± 0.07 g). Consistent with the *ob/ob* data, DIO mice that lack hepatocyte CaMKII γ had lower fasting insulin levels (Figure 1E), lower blood glucose levels (Figure 1F), and an improved blood glucose response to glucose challenge (Figure 1G). Similar results were found using a third model in which holo-CaMKII γ KO (*Camk2g^{-/-}*) mice were placed on the high fat diet (Figure S1A–B).

Consistent with an improvement insulin resistance, targeting hepatocyte CaMKII γ in obese mice (AAV8-TBG-Cre) led to a decrease in hepatic steatosis (Figure S1C); hepatocyte TG content was also decreased in the Cre-treated mice (79.13 ± 7.21 vs. 59.6 ± 7.27 mg/g liver). The decrease in hepatic steatosis was not due to an increase in triglyceride secretion, as the Cre-treated mice had a decrease in plasma triglyceride levels (266.78 ± 28.08 vs. 193.34 ± 13.01 mg/dl). These combined data suggest that hepatic CaMKII γ plays a central role in the manifestations of obesity-induced insulin resistance.

Although hepatic p38 activation has been implicated in insulin resistance in obese mice (Hemi et al., 2011), the upstream and downstream mechanisms remain incompletely understood. We have previously shown that CaMKII regulates p38 α MAPK activity in hepatocytes (Ozcan et al., 2012), and so we explored the possibility that p38 might also function as a downstream mediator of CaMKII in the pathogenesis of insulin resistance. To this end, the gene encoding p38 α (*Mapk14*) was silenced in hepatocytes by injecting DIO *Mapk14^{fl/fl}* mice with AAV-TBG-Cre, which led to more than 90% silencing of p38 α protein levels in liver (below) without affecting body weight (41 ± 2.36 vs. 39 ± 1.04 g), food intake (2.62 ± 0.09 vs. 2.24 ± 0.06 g per mouse per day) or epididymal fat pad mass (1.92 ± 0.15 vs. 1.83 ± 0.14 g). Compared with control mice (AAV-TBG-LacZ), mice

deficient in hepatocyte p38 α had lower fasting blood glucose (Figure 2A), lower plasma insulin levels (Figure 2B), improved blood glucose response to glucose challenge and enhanced glucose disposal upon insulin stimulation (Figure 2C&D).

MAPK-activating protein kinase 2 (MK2) is a well-characterized downstream effector of p38 (Freshney et al., 1994; Rouse et al., 1994). Moreover, activated MK2 forms a tight complex with p38 α and thus reciprocally stabilizes p38 α (Gaestel, 2006). To investigate the role of MK2, *ob/ob* mice were injected i.v. with adenovirus encoding MK2 with a mutation in its p38 phosphorylation site (T222A), which acts as a dominant negative (DN) form of the enzyme (Streicher et al., 2010). This treatment resulted in lowering of blood glucose (Figure 2E), plasma insulin levels (Figure 2F), and a marked improvement in glucose tolerance (Figure 2G), without changing body weight (49.4 ± 2.01 vs. 51.4 ± 0.67 g) or food intake (5.37 ± 0.44 vs. 5.52 ± 0.23 g per mouse per day). Thus, liver p38 α and MK2, like CaMKII, play an important role in the development of hyperglycemia and hyperinsulinemia in obese mice and the response of these mice to exogenous glucose.

Deletion or Inhibition of CaMKII, p38 α , or MK2 Improves Insulin-Induced Akt Phosphorylation in Obese Mice

In view of the above data, we focused our attention on hepatocyte insulin signaling, where defects contribute to insulin resistance in obesity (Brown and Goldstein, 2008). As a measure of hepatic insulin signaling, we assayed pSer⁴⁷³-Akt in the livers of mice injected with insulin through the portal vein. The data show a significant increase in insulin-induced p-Akt in the livers of *Camk2g*^{-/-} DIO mice compared with WT DIO mice (Figure 3A, **top 2 blots**). Improvements in Akt phosphorylation are often associated with increased tyrosine phosphorylation of IR and/or IRS-1/2. However, in the case of DIO CaMKII KO mice, neither phosphorylation of IR (data not shown) nor IRS-1 was increased (Figure 3A, **bottom 2 blots**). Similar results were found in DIO *Camk2g*^{fl/fl} mice injected with AAV-TBG-Cre and in *ob/ob* mice treated with dominant-negative adeno-K43A-CaMKII: insulin-induced phosphorylation of Akt was increased but phosphorylation of IR and IRS-1 was not (Figure 3B and S2A). Note that inhibition of CaMKII in chow-fed lean mice did not induce significant changes in p-Akt levels (Figure S2B), indicating a specific role of CaMKII in defective insulin-induced p-Akt in obese mice.

The data in Figure 2 showed that liver-directed silencing of either p38, which is a downstream target of CaMKII, or MK2, which is a substrate and stabilizer of p38, improved plasma insulin and response to glucose and insulin. To link these findings to hepatic insulin signaling, we treated DIO *Mapk14*^{fl/fl} mice with AAV-TBG-Cre and then assayed insulin-induced p-Akt. As with CaMKII silencing, there was enhanced insulin-stimulated Akt phosphorylation without an increase in IR or IRS-1/2 phosphorylation (Figure 3C). Similarly, Akt activation was increased in *ob/ob* mice injected with dominant-negative adeno-T222A-MK2 (Figure S2C) without an increase in the phosphorylation of IR or IRS proteins (data not shown). These combined data indicate that CaMKII, p38 α , and MK2 participate in defective insulin-p-Akt signaling in the livers of obese mice at a step to distal to IRS phosphorylation.

Inhibition of CaMKII or p38 α Improves Insulin-Induced Akt Phosphorylation distal to IR and IRS and in a FoxO1-Independent Manner

To further probe mechanism, we moved to a primary murine hepatocyte (HC) model in which insulin-induced Akt phosphorylation is suppressed by treatment with the saturated fatty acid palmitate (Achard and Laybutt, 2012). Using transduction with adeno-K43A-CaMKII, we first showed that this model recapitulates the improvement in insulin-induced Akt phosphorylation conferred by inhibition of CaMKII (Figure 4A, **top 3 blots**), whereas

adeno-K43A-CaMKII transduction did not evoke any significant changes under control, BSA treated group. Moreover, consistent with our *in vivo* findings, CaMKII inhibition did not enhance Tyr-phosphorylation of IRS-1 (Figure 4A, **right panel**), IR, or IRS-2 (data not shown). Similar data were obtained using p38 α -deficient hepatocytes in terms of p-Akt (Figure 4B, **upper panel, top 3 blots**) and p-IR and p-IRS-1 (Figure 4B, **left lower panel**). Consistent with improved Akt activation, insulin-stimulated phosphorylation of the downstream Akt targets, FoxO1 and GSK-3 β , were also significantly improved (Figure 4B, **right lower panel, bottom 4 blots**) and glucose output was significantly inhibited (49.97 ± 2.76 vs. 82.78 ± 4.66 nmol per hour per mg protein). Furthermore, in order to acquire information about the human relevance of our murine HC studies, we tested the effect of CaMKII inhibition in metabolism-qualified human HCs using the palmitate model. Consistent with our murine HC data, palmitate-induced suppression of insulin-induced p-Akt was prevented by CaMKII inhibition using adeno-K43A-CaMKII (Figure 4C).

We next examined whether a constitutively active mutant of CaMKII (CA-CaMKII) is sufficient to interfere with insulin action in the absence of palmitate. This mutant possesses an amino acid substitution, T287D, which mimics autophosphorylation at T287 and results in autonomous activity in the absence of bound calcium/calmodulin (Ozcan et al., 2012; Pfeleiderer et al., 2004). The data show that CA-CaMKII resulted in a decrease in insulin-induced Akt phosphorylation without decreasing either p-IRS-1, which was actually increased, or p-IRS-2 (Figure 4D). Thus, CaMKII is both necessary and sufficient for the palmitate-induced insulin signaling defect in primary HCs.

We recently demonstrated that CaMKII mediates glucagon-induced hepatic glucose production (HGP) through p38-induced phosphorylation of FoxO1 (Ozcan et al., 2012). In particular, phosphorylation of FoxO1 by p38 promotes nuclear localization of FoxO1 and transcription of FoxO1 target genes involved in HGP, and inhibition of CaMKII or p38 leads to cytoplasmic localization of FoxO1 and inhibition of HGP. Because FoxO1 has been implicated in the regulation of Akt action (Lin and Accili, 2011), we investigated the contribution of FoxO1 nuclear exclusion in the enhancement of insulin signaling by CaMKII deficiency. We began with a series of experiments using nuclear FoxO1 restoration in palmitate-treated HCs. First, a nuclear FoxO1 bioassay—induction of the FoxO1 gene target *Igfb1*—was used to verify our previous data (Ozcan et al., 2012) that deletion of CaMKII γ caused a decrease in nuclear FoxO1 activity that could be restored by transduction with constitutively nuclear adeno-FoxO1-ADA (Figure S3A). We then used this model to ask whether FoxO1 restoration would abrogate the benefit of CaMKII deletion on insulin-induced p-Akt. As before, deletion of CaMKII improved insulin-induced p-Akt, and this improvement was not diminished by FoxO1 restoration (Figure S3B). These data indicate the distinct nature of the two CaMKII pathways.

We next investigated this important point *in vivo*. As in lean mice, adeno-K43A-CaMKII treatment markedly diminished nuclear FoxO1 in the livers of obese mice (Figure S3C). However, as was the case with HCs, restoration of nuclear FoxO1 did not reverse the benefit of CaMKII inhibition (K43A) on insulin-induced p-Akt (Figure S3D). Thus, the improvement in insulin-induced p-Akt by CaMKII deficiency is not due to nuclear exclusion of FoxO1. Rather, there appear to be two separate CaMKII pathways, one involved in CaMKII-p38-FoxO1 dependent HGP (Ozcan et al., 2012) and the other involved in defective insulin-induced p-Akt.

Inhibition of CaMKII or p38 α Improves Insulin-Induced Akt Phosphorylation by Suppressing TRB3

In considering mechanisms of how insulin-induced p-Akt signaling distal to IRS proteins is regulated, we tested the role of the pseudokinase tribble 3 (TRB3), a molecule that is

increased in the livers of obese mice and humans and previously shown to bind to Akt and thereby prevent its phosphorylation by insulin (Du et al., 2003). We first investigated the effect of CaMKII and p38 deficiency on TRB3 levels in HCs. Palmitate treatment of control HCs led to an increase in TRB3 levels, consistent with a previous report (Cunha et al., 2012). Most importantly, CaMKII deficiency markedly decreased TRB3 protein and mRNA under both basal and palmitate-treated conditions (Figure 5A and S4A). To show relevance *in vivo*, we tested the effect of CaMKII deficiency or inhibition on TRB3 levels in obese mice. Consistent with the HC data, TRB3 levels were markedly suppressed in DIO *Camk2g*^{-/-} mice or in *ob/ob* mice transduced with adeno-K43A-CaMKII (Figure 5B).

To test the importance of TRB3 in the enhancement of insulin-induced p-Akt conferred by CaMKII deficiency, we transduced DIO *Camk2g*^{fl/fl} mice with TRB3 in order to bring TRB3 protein to a level similar to that in WT. TRB3 overexpression abrogated the improvement in insulin-induced p-Akt conferred by CaMKII deficiency (Figure S4B), indicating that the suppression of TRB3 by CaMKII deficiency is causally important in the improvement in insulin signaling. We then conducted a similar experiment except used physiologic re-feeding (16 h fasting followed by 4 h of a high-fat diet) instead of portal vein insulin injection to activate Akt. Similar to the case with portal vein insulin injections, TRB3 overexpression abolished the improvement in re-feeding-induced p-Akt conferred by CaMKII inhibition (Figure 5C). In line with the effect of TRB3 restoration on insulin signaling, treatment of mice with adeno-TRB3 abrogated the lowering of blood glucose (Figure 5D) and plasma insulin (Figure 5E) by CaMKII inhibition in DIO mice under both fasting and re-feeding conditions. Next, we sought to examine the effect of CaMKII deletion in TRB3-inhibited HCs. RNAi mediated knock down of TRB3 in CaMKII-deficient HCs did not further improve insulin-induced p-Akt (Figure S4C), consistent with the idea that TRB3 is the downstream effector of CaMKII in the regulation of insulin-induced p-Akt.

The data in our previous report (Ozcan et al., 2012) and here indicate that, in the setting of obesity, CaMKII γ deficiency lowers HGP by suppressing p38-mediated FoxO1 nuclear localization and improves insulin signaling by suppressing hepatic TRB3 expression, which then leads to improvement in insulin/Akt signaling. Although we showed above that nuclear FoxO1 does not affect insulin-induced p-Akt, an interesting question is whether the improvement in p-Akt (new pathway here) contributes, via Akt phosphorylation sites on FoxO1 (Lin and Accili, 2011), to nuclear exclusion of FoxO1 in obese mice lacking CaMKII or p38, which is promoted by decreased p38-mediated phosphorylation of FoxO1 (Ozcan et al., 2012). To address this issue, we disabled the improvement in p-Akt in CaMKII-deficient obese mice through TRB3 restoration (above). As predicted by the idea that both pathways contribute to the exclusion of nuclear FoxO1 by CaMKII deficiency in the setting of obesity, TRB3 restoration in CaMKII-deficient mice led to a partial increase in nuclear FoxO1 (Figure S4D). We then reasoned that we should be able to show no effect of TRB3 on nuclear FoxO1 if we chose a non-insulin resistant model, *i.e.*, a model where TRB3 would be irrelevant in terms of the Akt-FoxO1 pathway. For this purpose, we used non-insulin-resistant forskolin-treated HCs (Ozcan et al., 2012). Nuclear FoxO1 biological activity was assayed by quantifying the mRNA levels of the FoxO1 target genes, *G6pc* and *Pck1*. In this case, as predicted, the suppressive effect of CaMKII γ deficiency on forskolin-induced *G6Pc* and *Pck1* mRNA was not abrogated by transduction with adeno-TRB3 (Figure S4E). Thus, in the absence of a defect in insulin signaling, TRB3 restoration does not affect the ability of CaMKII deficiency to suppress HGP gene induction. These data further establish the separateness of the two CaMKII/p38 pathways, although in the setting of insulin resistance, FoxO1 nuclear localization is promoted by both pathways.

CaMKII Deficiency Suppresses TRB3 by Decreasing ER Stress-Induced ATF4

TRB3 expression has been reported to be increased in cancer cells and pancreatic islets undergoing endoplasmic reticulum (ER) stress (Bromati et al., 2011; Corcoran et al., 2005). Moreover, in HEK293 embryonic kidney cells treated with tunicamycin, a glycosylation inhibitor that activates the UPR, TRB3 was shown to be a direct transcriptional target of the ER stress-inducible transcription factor ATF4 (Ohoka et al., 2005). Because hepatic ER stress is increased obesity and may act as a link between obesity and insulin resistance (Gregor et al., 2009; Ozcan et al., 2004), we reasoned that a CaMKII-ATF4-TRB3 pathway might be upstream of defective insulin-induced p-Akt in obese liver. We first measured ATF4 levels in WT vs. CaMKII γ -deficient HCs under various conditions. Exposure to tunicamycin increased ATF4 in control HCs but not in CaMKII-deficient HCs (Figure 6A). Similarly, the livers of obese mice deficient in hepatic CaMKII γ had lower ATF4 levels compared with obese WT mice (Figure 6B), suggesting that CaMKII might be suppressing TRB3 by first suppressing ATF4. To test this possibility and link it to insulin-induced p-Akt, palmitate-treated CaMKII γ -deficient HCs were transduced with adeno-ATF4 to restore the level of this protein to the WT level. Consistent with our hypothesis, ATF4 restoration resulted in an increase in TRB3 mRNA and protein levels and abrogation of the improvement in p-Akt seen with CaMKII deficiency (Figure 6C–D). To further validate the importance of ATF4 suppression in the improvement of insulin signaling by CaMKII deficiency, we restored ATF4 in adeno-K43A-CaMKII-treated DIO mice. We observed that the beneficial effect of CaMKII γ inhibition on insulin-induced p-Akt was abrogated by transduction with adeno-ATF4 (Figure 6E). Consistent with the effect of ATF4 restoration on insulin signaling, the blood glucose- and plasma insulin-lowering effect of CaMKII inhibition in DIO mice was also abrogated by adeno-ATF4 (Figure 6F). These data support a signaling pathway in which CaMKII promotes ATF4 expression, which in turn induces TRB3, leading to suppression of insulin-induced p-Akt.

ATF4 is translationally up-regulated when the PERK branch of the ER stress unfolded protein response (UPR) is activated (Tabas and Ron, 2011; Walter and Ron, 2011). We therefore investigated whether CaMKII deficiency suppresses the PERK branch of UPR as a mechanism for reduced ATF-4 and TRB3 expression. When exposed to tunicamycin, HCs lacking CaMKII γ showed a marked decrease in PERK phosphorylation, which is a measure of its activation, as well as decreased expression of the ATF4 gene target CEBP β -homologous protein (CHOP) (Figure S5A). Similar results were seen with tunicamycin- or palmitate-treated HCs deficient in CaMKII γ or p38 α (Figures S5B and S5C). To explore a possible role of CaMKII in the regulation of PERK branch of UPR *in vivo*, we analyzed *Chop* mRNA levels in obese mice. Consistent with our *in vitro* data, obese mice deficient in hepatic CaMKII had lower *Chop* mRNA levels in liver compared with WT mice (Figure S5D). Interestingly, the IRE1 α branch of the UPR, as measured by *Xbp1* mRNA splicing, was not activated in either palmitate-treated HCs or in obese mouse liver (Figure S5E–F). Thus, CaMKII deficiency selectively suppresses the PERK branch of the UPR in the setting of obesity, leading to decreased ATF4 and TRB3 and increased insulin-induced p-Akt.

Evidence that an ATF6-p58^{IPK} Pathway is Upstream of the ATF4-TRB3-Akt Pathway

We next addressed how silencing of CaMKII might suppress the PERK branch of the UPR. While global suppression of ER stress would be a theoretical possibility, we instead focused on the idea that CaMKII deficiency might increase the expression of a widely studied inhibitor of PERK kinase called p58^{IPK} (Yan et al., 2002). Initial support for this idea came from the finding that p58^{IPK} mRNA and protein levels were increased by CaMKII γ or p38 α deficiency in ER-stressed HCs and obese mice liver (Figures 7A and S6A–C). Most importantly, siRNA-mediated silencing of p58^{IPK} increased *Trb3* and abrogated the improvement in insulin-Akt signaling in CaMKII-deficient, palmitate-treated HCs (Figure

7B–C), demonstrating a casual link between the proposed upstream role of p58^{IPK} and the key functional endpoint of the CaMKII pathway, insulin-induced p-Akt.

Finally, to explore how CaMKII deficiency might increase p58^{IPK} in obese mice liver, we explored the role of a known inducer of the molecule, ATF6, which has been shown to be decreased in the livers of obese mice (Wang et al., 2009; Wu et al., 2007). This hypothesis predicts that CaMKII deficiency would increase ATF6 levels, which indeed was the case in obese liver, in tunicamycin-treated HCs, and in palmitate-treated HCs (Figures 7D, S6D, and 7F). To determine causation, we silenced *Atf6* in palmitate-treated CaMKII-deficient HCs using siRNA and found that this treatment lowered *P58^{ipk}*, increased *Trb3*, and reduced insulin-induced p-Akt to the level of palmitate-treated control HCs (Figure 7E–F). Thus, inhibition of hepatic CaMKII improves insulin signaling in the setting of obesity through induction of ATF6 and p58^{IPK}, which suppresses a PERK-ATF4-TRB3 pathway.

DISCUSSION

The epidemic of obesity and T2D demands a precise understanding of the molecular events that link obesity to the two cardinal features of T2D, hyperglycemia and insulin resistance. The current findings, viewed together with our two recent studies (Ozcan et al., 2012; Wang et al., 2012), presents a unified scheme in which cytosolic calcium working through CaMKII in the liver plays a central role (Figure 7G). Cytosolic calcium in the liver is elevated in obesity through at least two mechanisms: lipid-induced de-activation of the calcium pump SERCA (Fu et al., 2011; Park et al., 2010) and opening of the IP3R ER calcium channel by two processes triggered by glucagon receptor activation: formation of IP3 by phospholipase C (Hansen et al., 1998) and direct activation of the channel by PKA-mediated phosphorylation of IP3R (Wang et al., 2012). With regard to excessive HGP as a cause of hyperglycemia, the released calcium activates both calcineurin, which promotes nuclear localization of CRT2 (Wang et al., 2012), and CaMKII, which, through p38, promotes nuclear by localization of FoxO1 (Ozcan et al., 2012). The current report reveals that a separate pathway in the liver, also mediated by CaMKII-p38, disrupts insulin-induced Akt phosphorylation, which is a key process in the pathogenesis of insulin resistance (Brozinick et al., 2003; Cho et al., 2001; Krook et al., 1998). From a translational viewpoint, this scheme suggests that a single pathway could be therapeutically inhibited to achieve improvement in both hyperglycemia and insulin resistance in obesity and T2D.

The key downstream step through which CaMKII deficiency improves insulin-induced p-Akt is suppression of TRB3, which binds Akt, prevents its membrane association, and thus block its phosphorylation (Du et al., 2003). TRB3 levels are increased in the livers of obese mice and humans, and it is proposed to play a major role in hepatic insulin resistance in this setting (Du et al., 2003; Lima et al., 2009). Notably, when TRB3 is expressed in WT mouse liver to a level similar to that in obese mouse liver, insulin resistance occurs, whereas silencing its expression in obesity improves glucose tolerance (Du et al., 2003). Moreover, a common gain-of-function polymorphism in TRB3 (Q48R) that increases the ability of TRB3 to suppress insulin-induced p-Akt is associated with increased insulin resistance in T2D in several independent cohorts (Prudente et al., 2005). TRB3 may also play a role in adipose tissue, because TRB3 antisense oligonucleotide (ASO) treatment of obese rats was reported to improve insulin sensitivity through a mechanism that involved activation of PPAR- γ and changes in adipogenesis rather than an increase in p-Akt (Weismann et al., 2011). In the case of the CaMKII pathway, the hepatic p-Akt mechanism is clearly important, but whether changes in PPAR γ and adipogenesis also occur remains to be investigated.

An important finding in our study is that CaMKII induces TRB3 through activation of the PERK-ATF4 branch of UPR, providing a novel link between CaMKII and ER stress. In the

context of previous findings linking P58IPK to suppression of PERK activation (Yan et al., 2002), our data suggest that the obesity-induced CaMKII/P38 pathway activates PERK through suppression of p58^{IPK}. Interestingly, p58^{IPK}-deficient mice exhibit glucosuria and hyperglycemia through a mechanism attributed to β -cell dysfunction (Ladiges et al., 2005). Our results now reveal another potential beneficial effect of p58^{IPK} in metabolism, namely, improvement in hepatic insulin signaling through suppression of CaMKII-induced ATF4 and TRB3.

We show that a key link between CaMKII/p38 deficiency and de-activation of the PERK branch of the UPR is activation of an ATF6-p58^{IPK} pathway. CaMKII-deficient obese mice have higher nuclear ATF6 levels, and silencing ATF6 in these mice lowers p58^{IPK} and suppresses insulin-induced p-Akt. How inhibition of the CaMKII/p38 pathway leads to increased ATF6 expression remains to be elucidated, but it is interesting to consider previous studies linking CaMKII/p38 activation with changes in gene expression (Backs et al., 2006; Raingeaud et al., 1996). As with p58^{IPK} induction and TRB3 suppression, ATF6 activation may have additional and independent beneficial effects in obesity and T2D. In particular, Montminy and colleagues have provided evidence that ATF6 could suppress HGP through disruption of CREB-CRTC2 interaction (Wang et al., 2009).

The discovery of a common pathway that independently affects the two cardinal features of T2D raises the possibility of new therapeutic targets. To the extent that excessive glucagon signaling is at least one mechanism that likely activates the CaMKII-p38-MK2 pathway in T2D, relevance to humans is suggested by the ability of glucagon receptor antagonists (GRAs) to markedly lower blood sugar in human subjects (Petersen and Sullivan, 2001). However, there may be an advantage to targeting a more downstream branch of the glucagon pathway in order to avoid the possible adverse effects of GRAs (Yang et al., 2011). In terms of the “druggability” of the molecules in the pathway, CaMKII inhibitors are in development for heart failure (Rokita and Anderson, 2012), and MK2 inhibitors are being explored as a more effective alternative than p38 inhibitors for inflammatory diseases (Huang et al., 2012). Because all new diabetes drugs must pass safety tests for coronary artery disease, the applications of these inhibitors to T2D may be particularly advantageous: CaMKII inhibition in liver lowers plasma cholesterol and triglycerides in obese mice; CaMKII inhibition in macrophages protects the cells from ER stress-induced apoptosis, a key step in advanced plaque progression (Timmins et al., 2009); and MK2-deficient *Ldlr*^{-/-} mice are protected against atherosclerosis (Jagavelu et al., 2007).

EXPERIMENTAL PROCEDURES

Mouse Experiments

Camk2g^{-/-} were generated as described previously (Backs et al., 2010) and crossed onto the C57BL6/J background. *Camk2g*^{fl/fl} mice were generated by flanking exon 1–2 with *loxP* sites, which will be described in detail elsewhere (M. Kreußner *et al.*, submitted manuscript), and then crossed onto the C57BL6/J background. *Ob/ob* mice were obtained from Jackson Labs. *Mapk14*^{fl/fl} mice were generated as described previously (Engel et al., 2005) and generously provided by Dr. Yibin Wang, UCLA School of Medicine. Male mice were fed a standard chow diet or a high-fat diet with 60% kcal from fat (Research Diets) and maintained on a 12-h-light-dark cycle. Recombinant adenovirus ($0.5\text{--}3 \times 10^9$ plaque-forming units/mice) was delivered by tail vein injection, and experiments were commenced after 5–7 days. Fasting blood glucose was measured in mice that were fasted for 4–6 h, with free access to water, using a glucose meter. Glucose tolerance tests were performed in overnight-fasted mice by assaying blood glucose at various times after i.p. injection of glucose (0.5 g/kg for *ob/ob* and 1.5 g/kg for DIO). Plasma insulin levels were measured using ultra-sensitive mouse insulin ELISA Kit (Crystal Chem). Insulin tolerance tests were

performed in 5 h-fasted mice by assaying blood glucose at various times after i.p. injection of insulin (2 IU/kg for *ob/ob* and 0.75–1 IU/kg for DIO). Animal studies were performed in accordance with the Columbia University Institutional Animal Care and Use Committee.

Portal Vein Insulin Infusion and Protein Extraction from Tissues

Following 6 h food withdrawal, mice were anesthetized, and insulin (1–2 IU/kg) or PBS was injected into mice through the portal vein. Three minutes after injection, tissues were removed, frozen in liquid nitrogen, and kept at 80°C until processing. For protein extraction, tissues were placed in a cold lysis buffer (25 mM Tris-HCl pH 7.4, 1 mM EGTA, 1 mM EDTA, 10 mM Na₄P₂O₇, 10 mM NaF, 2 mM Na₃VO₄, 1% NP-40, 2 mM PMSF, 5 µg/ml leupeptin, 10 nM okadaic acid, and 5 µg/ml aprotinin). After homogenization on ice, the tissue lysates were centrifuged, and the supernatant fractions were used for immunoblot analysis.

Primary Hepatocytes (HCs)

Primary mouse HCs were isolated from 8- to 12-week-old mice as described previously (Ozcan et al., 2012). For most experiments, the HCs were cultured in DMEM containing 10% fetal bovine serum, treated as described in the figure legends, and then incubated for 5 h in serum-free DMEM. HCs were transduced with adenoviral constructs 4 h after plating, and experiments were conducted 12 h after transduction. Transfections with scrambled RNA and siRNAs targeting *p58^{ipk}* and *Atf6* were carried out using Lipofectamine RNAiMAX transfection reagent (Life Technologies, Inc.) according to manufacturer's instructions. Metabolism-qualified human HCs were purchased from Life Technologies and cultured according to the manufacturer's instructions.

Statistical Analysis

All results are presented as mean ± SEM. P values were calculated using the Student's t-test for normally distributed data and the Mann-Whitney rank sum test for non-normally distributed data.

Supplementary Material

Refer to Web version on PubMed Central for supplementary material.

Acknowledgments

We thank Dr. Harold A. Singer (Albany Medical College) for adeno-LacZ, T287A-CaMKII, K43A-CaMKII; Dr. Marc Montminy (Salk Institute for Biological Studies) for adeno-TRB3 and - TRB3 RNAi; Randal J. Kaufman (Sanford-Burnham Medical Research Institute) for adeno-ATF4; and Dr. Domenico Accili (Columbia University) for adeno-FoxO1-ADA. This work was supported by American Heart Association Scientist Development Grant (11SDG5300022) and NYONRC Pilot and Feasibility Grant (DK26687) to L.O.; by FAPESP/BEPE 2012/21290-4 to J.C.S.; by the DZHK (German Centre for Cardiovascular Research), BMBF (German Ministry of Education and Research), DFG (Deutsche Forschungsgemeinschaft; BA 2258/2-1), and the European Commission (FP7-Health-2010; MEDIA-261409) to J.B.; and NIH grants HL087123 and HL075662 to I.T. Drs. Ozcan and Tabas are in the group of co-founders of Tabomedex Biosciences LLC, which is developing inhibitors of the pathway described in this report for treatment of type 2 diabetes.

References

Achard CS, Laybutt DR. Lipid-induced endoplasmic reticulum stress in liver cells results in two distinct outcomes: adaptation with enhanced insulin signaling or insulin resistance. *Endocrinology*. 2012; 153:2164–2177. [PubMed: 22374970]

- Backs J, Song K, Bezprozvannaya S, Chang S, Olson EN. CaM kinase II selectively signals to histone deacetylase 4 during cardiomyocyte hypertrophy. *J Clin Invest.* 2006; 116:1853–1864. [PubMed: 16767219]
- Backs J, Stein P, Backs T, Duncan FE, Grueter CE, McAnally J, Qi X, Schultz RM, Olson EN. The gamma isoform of CaM kinase II controls mouse egg activation by regulating cell cycle resumption. *Proc Natl Acad Sci U S A.* 2010; 107:81–86. [PubMed: 19966304]
- Bornfeldt KE, Tabas I. Insulin resistance, hyperglycemia, and atherosclerosis. *Cell Metab.* 2011; 14:575–585. [PubMed: 22055501]
- Bromati CR, Lellis-Santos C, Yamanaka TS, Nogueira TC, Leonelli M, Caperuto LC, Gorjao R, Leite AR, Anhe GF, Bordin S. UPR induces transient burst of apoptosis in islets of early lactating rats through reduced AKT phosphorylation via ATF4/CHOP stimulation of TRB3 expression. *Am J Physiol Regul Integr Comp Physiol.* 2011; 300:R92–100. [PubMed: 21068199]
- Brown MS, Goldstein JL. Selective versus total insulin resistance: a pathogenic paradox. *Cell Metab.* 2008; 7:95–96. [PubMed: 18249166]
- Brozinick JT Jr, Roberts BR, Dohm GL. Defective signaling through Akt-2 and -3 but not Akt-1 in insulin-resistant human skeletal muscle: potential role in insulin resistance. *Diabetes.* 2003; 52:935–941. [PubMed: 12663464]
- Cho H, Mu J, Kim JK, Thorvaldsen JL, Chu Q, Crenshaw EB 3rd, Kaestner KH, Bartolomei MS, Shulman GI, Birnbaum MJ. Insulin resistance and a diabetes mellitus-like syndrome in mice lacking the protein kinase Akt2 (PKB beta). *Science.* 2001; 292:1728–1731. [PubMed: 11387480]
- Corcoran CA, Luo X, He Q, Jiang C, Huang Y, Sheikh MS. Genotoxic and endoplasmic reticulum stresses differentially regulate TRB3 expression. *Cancer Biol Ther.* 2005; 4:1063–1067. [PubMed: 16294033]
- Cunha DA, Igoillo-Esteve M, Gurzov EN, Germano CM, Naamane N, Marhfour I, Fukaya M, Vanderwinden JM, Gysemans C, Mathieu C, Marselli L, Marchetti P, Harding HP, Ron D, Eizirik DL, Cnop M. Death protein 5 and p53-upregulated modulator of apoptosis mediate the endoplasmic reticulum stress-mitochondrial dialog triggering lipotoxic rodent and human beta-cell apoptosis. *Diabetes.* 2012; 61:2763–2775. [PubMed: 22773666]
- Du K, Herzig S, Kulkarni RN, Montminy M. TRB3: a tribbles homolog that inhibits Akt/PKB activation by insulin in liver. *Science.* 2003; 300:1574–1577. [PubMed: 12791994]
- Engel FB, Schebesta M, Duong MT, Lu G, Ren S, Madwed JB, Jiang H, Wang Y, Keating MT. p38 MAP kinase inhibition enables proliferation of adult mammalian cardiomyocytes. *Genes Dev.* 2005; 19:1175–1187. [PubMed: 15870258]
- Freshney NW, Rawlinson L, Guesdon F, Jones E, Cowley S, Hsuan J, Saklatvala J. Interleukin-1 activates a novel protein kinase cascade that results in the phosphorylation of Hsp27. *Cell.* 1994; 78:1039–1049. [PubMed: 7923354]
- Fu S, Yang L, Li P, Hofmann O, Dicker L, Hide W, Lin X, Watkins SM, Ivanov AR, Hotamisligil GS. Aberrant lipid metabolism disrupts calcium homeostasis causing liver endoplasmic reticulum stress in obesity. *Nature.* 2011; 473:528–531. [PubMed: 21532591]
- Gaestel M. MAPKAP kinases - MKs - two's company, three's a crowd. *Nat Rev Mol Cell Biol.* 2006; 7:120–130. [PubMed: 16421520]
- Gregor MF, Yang L, Fabbrini E, Mohammed BS, Eagon JC, Hotamisligil GS, Klein S. Endoplasmic reticulum stress is reduced in tissues of obese subjects after weight loss. *Diabetes.* 2009; 58:693–700. [PubMed: 19066313]
- Hansen LH, Gromada J, Bouchelouche P, Whitmore T, Jelinek L, Kindsvogel W, Nishimura E. Glucagon-mediated Ca²⁺ signaling in BHK cells expressing cloned human glucagon receptors. *Am J Physiol.* 1998; 274:C1552–1562. [PubMed: 9611120]
- Hemi R, Yochananov Y, Barhod E, Kasher-Meron M, Karasik A, Tirosh A, Kanety H. p38 mitogen-activated protein kinase-dependent transactivation of ErbB receptor family: a novel common mechanism for stress-induced IRS-1 serine phosphorylation and insulin resistance. *Diabetes.* 2011; 60:1134–1145. [PubMed: 21386087]
- Huang X, Zhu X, Chen X, Zhou W, Xiao D, Degrado S, Aslanian R, Fossetta J, Lundell D, Tian F, Trivedi P, Palani A. A three-step protocol for lead optimization: quick identification of key

- conformational features and functional groups in the SAR studies of non-ATP competitive MK2 (MAPKAPK2) inhibitors. *Bioorg Med Chem Lett.* 2012; 22:65–70. [PubMed: 22169260]
- Jagavelu K, Tietge UJ, Gaestel M, Drexler H, Schieffer B, Bavendiek U. Systemic deficiency of the MAP kinase-activated protein kinase 2 reduces atherosclerosis in hypercholesterolemic mice. *Circ Res.* 2007; 101:1104–1112. [PubMed: 17885219]
- Kerouz NJ, Horsch D, Pons S, Kahn CR. Differential regulation of insulin receptor substrates-1 and -2 (IRS-1 and IRS-2) and phosphatidylinositol 3-kinase isoforms in liver and muscle of the obese diabetic (ob/ob) mouse. *J Clin Invest.* 1997; 100:3164–3172. [PubMed: 9399964]
- Konner AC, Bruning JC. Selective insulin and leptin resistance in metabolic disorders. *Cell Metab.* 2012; 16:144–152. [PubMed: 22883229]
- Krook A, Roth RA, Jiang XJ, Zierath JR, Wallberg-Henriksson H. Insulin-stimulated Akt kinase activity is reduced in skeletal muscle from NIDDM subjects. *Diabetes.* 1998; 47:1281–1286. [PubMed: 9703329]
- Ladiges WC, Knoblaugh SE, Morton JF, Korth MJ, Sopher BL, Baskin CR, MacAuley A, Goodman AG, LeBoeuf RC, Katze MG. Pancreatic beta-cell failure and diabetes in mice with a deletion mutation of the endoplasmic reticulum molecular chaperone gene P58IPK. *Diabetes.* 2005; 54:1074–1081. [PubMed: 15793246]
- Leavens KF, Birnbaum MJ. Insulin signaling to hepatic lipid metabolism in health and disease. *Crit Rev Biochem Mol Biol.* 2011; 46:200–215. [PubMed: 21599535]
- Lima AF, Ropelle ER, Pauli JR, Cintra DE, Frederico MJ, Pinho RA, Velloso LA, De Souza CT. Acute exercise reduces insulin resistance-induced TRB3 expression and amelioration of the hepatic production of glucose in the liver of diabetic mice. *J Cell Physiol.* 2009; 221:92–97. [PubMed: 19492410]
- Lin HV, Accili D. Hormonal regulation of hepatic glucose production in health and disease. *Cell Metab.* 2011; 14:9–19. [PubMed: 21723500]
- Ohoka N, Yoshii S, Hattori T, Onozaki K, Hayashi H. TRB3, a novel ER stress-inducible gene, is induced via ATF4-CHOP pathway and is involved in cell death. *EMBO J.* 2005; 24:1243–1255. [PubMed: 15775988]
- Ozcan L, Wong CC, Li G, Xu T, Pajvani U, Park SK, Wronska A, Chen BX, Marks AR, Fukamizu A, Backs J, Singer HA, Yates JR 3rd, Accili D, Tabas I. Calcium Signaling through CaMKII Regulates Hepatic Glucose Production in Fasting and Obesity. *Cell Metab.* 2012; 15:739–751. [PubMed: 22503562]
- Ozcan U, Cao Q, Yilmaz E, Lee AH, Iwakoshi NN, Ozdelen E, Tuncman G, Gorgun C, Glimcher LH, Hotamisligil GS. Endoplasmic reticulum stress links obesity, insulin action, and type 2 diabetes. *Science.* 2004; 306:457–461. [PubMed: 15486293]
- Park SW, Zhou Y, Lee J, Lee J, Ozcan U. Sarco(endo)plasmic reticulum Ca²⁺-ATPase 2b is a major regulator of endoplasmic reticulum stress and glucose homeostasis in obesity. *Proc Natl Acad Sci U S A.* 2010; 107:19320–19325. [PubMed: 20974941]
- Petersen KF, Sullivan JT. Effects of a novel glucagon receptor antagonist (Bay 27-9955) on glucagon-stimulated glucose production in humans. *Diabetologia.* 2001; 44:2018–2024. [PubMed: 11719833]
- Pfleiderer PJ, Lu KK, Crow MT, Keller RS, Singer HA. Modulation of vascular smooth muscle cell migration by calcium/calmodulin-dependent protein kinase II-delta 2. *Am J Physiol Cell Physiol.* 2004; 286:C1238–1245. [PubMed: 14761894]
- Prudente S, Hribal ML, Flex E, Turchi F, Morini E, De Cosmo S, Bacci S, Tassi V, Cardellini M, Lauro R, Sesti G, Dallapiccola B, Trischitta V. The functional Q84R polymorphism of mammalian Tribbles homolog TRB3 is associated with insulin resistance and related cardiovascular risk in Caucasians from Italy. *Diabetes.* 2005; 54:2807–2811. [PubMed: 16123373]
- Raingaud J, Whitmarsh AJ, Barrett T, Derijard B, Davis RJ. MKK3- and MKK6-regulated gene expression is mediated by the p38 mitogen-activated protein kinase signal transduction pathway. *Mol Cell Biol.* 1996; 16:1247–1255. [PubMed: 8622669]
- Rokita AG, Anderson ME. New therapeutic targets in cardiology: arrhythmias and Ca²⁺/calmodulin-dependent kinase II (CaMKII). *Circulation.* 2012; 126:2125–2139. [PubMed: 23091085]

- Rouse J, Cohen P, Trigon S, Morange M, Alonso-Llamazares A, Zamanillo D, Hunt T, Nebreda AR. A novel kinase cascade triggered by stress and heat shock that stimulates MAPKAP kinase-2 and phosphorylation of the small heat shock proteins. *Cell*. 1994; 78:1027–1037. [PubMed: 7923353]
- Saad MJ, Araki E, Miralpeix M, Rothenberg PL, White MF, Kahn CR. Regulation of insulin receptor substrate-1 in liver and muscle of animal models of insulin resistance. *J Clin Invest*. 1992; 90:1839–1849. [PubMed: 1331176]
- Saltiel AR, Kahn CR. Insulin signalling and the regulation of glucose and lipid metabolism. *Nature*. 2001; 414:799–806. [PubMed: 11742412]
- Samuel VT, Shulman GI. Mechanisms for insulin resistance: common threads and missing links. *Cell*. 2012; 148:852–871. [PubMed: 22385956]
- Streicher JM, Ren S, Herschman H, Wang Y. MAPK-activated protein kinase-2 in cardiac hypertrophy and cyclooxygenase-2 regulation in heart. *Circ Res*. 2010; 106:1434–1443. [PubMed: 20339119]
- Sun Z, Miller RA, Patel RT, Chen J, Dhir R, Wang H, Zhang D, Graham MJ, Unterman TG, Shulman GI, Sztalryd C, Bennett MJ, Ahima RS, Birnbaum MJ, Lazar MA. Hepatic Hdac3 promotes gluconeogenesis by repressing lipid synthesis and sequestration. *Nat Med*. 2012; 18:934–942. [PubMed: 22561686]
- Tabas I, Ron D. Integrating the mechanisms of apoptosis induced by endoplasmic reticulum stress. *Nat Cell Biol*. 2011; 13:184–190. [PubMed: 21364565]
- Timmins JM, Ozcan L, Seimon TA, Li G, Malagelada C, Backs J, Backs T, Bassel-Duby R, Olson EN, Anderson ME, Tabas I. Calcium/calmodulin-dependent protein kinase II links ER stress with Fas and mitochondrial apoptosis pathways. *J Clin Invest*. 2009; 119:2925–2941. [PubMed: 19741297]
- Walter P, Ron D. The unfolded protein response: from stress pathway to homeostatic regulation. *Science*. 2011; 334:1081–1086. [PubMed: 22116877]
- Wang Y, Li G, Goode J, Paz JC, Ouyang K, Srean R, Fischer WH, Chen J, Tabas I, Montminy M. Inositol-1,4,5-trisphosphate receptor regulates hepatic gluconeogenesis in fasting and diabetes. *Nature*. 2012; 485:128–132. [PubMed: 22495310]
- Wang Y, Vera L, Fischer WH, Montminy M. The CREB coactivator CRTC2 links hepatic ER stress and fasting gluconeogenesis. *Nature*. 2009; 460:534–537. [PubMed: 19543265]
- Weismann D, Erion DM, Ignatova-Todorava I, Nagai Y, Stark R, Hsiao JJ, Flannery C, Birkenfeld AL, May T, Kahn M, Zhang D, Yu XX, Murray SF, Bhanot S, Monia BP, Cline GW, Shulman GI, Samuel VT. Knockdown of the gene encoding *Drosophila* tribbles homologue 3 (*Trib3*) improves insulin sensitivity through peroxisome proliferator-activated receptor- γ activation in a rat model of insulin resistance. *Diabetologia*. 2011; 54:935–944. [PubMed: 21190014]
- Wu J, Rutkowski DT, Dubois M, Swathirajan J, Saunders T, Wang J, Song B, Yau GD, Kaufman RJ. ATF6 α optimizes long-term endoplasmic reticulum function to protect cells from chronic stress. *Dev Cell*. 2007; 13:351–364. [PubMed: 17765679]
- Yan W, Frank CL, Korth MJ, Sopher BL, Novoa I, Ron D, Katze MG. Control of PERK eIF2 α kinase activity by the endoplasmic reticulum stress-induced molecular chaperone P58IPK. *Proc Natl Acad Sci U S A*. 2002; 99:15920–15925. [PubMed: 12446838]
- Yang J, MacDougall ML, McDowell MT, Xi L, Wei R, Zavadski WJ, Molloy MP, Baker JD, Kuhn M, Cabrera O, Treadway JL. Polyomic profiling reveals significant hepatic metabolic alterations in glucagon-receptor (GCGR) knockout mice: implications on anti-glucagon therapies for diabetes. *BMC Genomics*. 2011; 12:281. [PubMed: 21631939]

HIGHLIGHTS

- An obesity-activated CaMKII-p38 pathway in liver suppresses insulin-induced p-Akt
- CaMKII/p38 activates a PERK-ATF4-TRB3 pathway that blocks Akt phosphorylation
- Inhibition of CaMKII-p38 lowers blood glucose and plasma insulin in obese mice
- Knowledge of this pathway suggests possible new therapeutic targets for diabetes

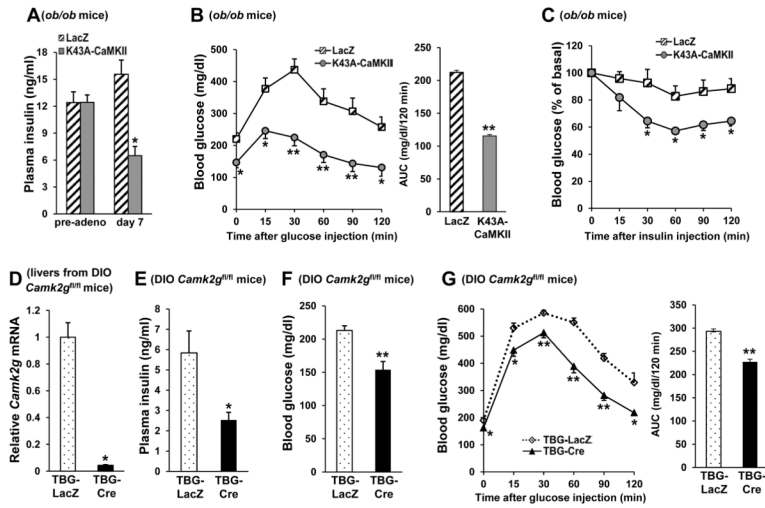


Figure 1. Inhibition or Deletion of Liver CaMKII γ Lowers Plasma Insulin and Improves Response to Glucose and Insulin Challenge in Obese Mice

(A) 9-wk-old *ob/ob* mice were fasted for 6 h, assayed for plasma insulin (“pre-adenovirus”), and then injected with adeno-LacZ (n=6) or -K43A-CaMKII (n=6). Seven days later, after a 6 h fast, the mice were assayed again for plasma insulin (“day 7”) (*p < 0.05, **p < 0.01; mean \pm S.E.M.). (B) Glucose tolerance tests were performed after overnight fasting (*p < 0.05, **p < 0.01; mean \pm S.E.M.). Area under the curve (AUC) is quantified in the right panel (**p < 0.01; mean \pm S.E.M.). (C) Insulin tolerance tests were performed after 6 h fasting (*p < 0.05; mean \pm S.E.M.). (D–G) Liver *Camk2g* mRNA, fasting plasma insulin, fasting blood glucose and blood glucose after glucose challenge in DIO *Camk2g^{fl/fl}* mice after treatment with adeno-associated virus (AAV) containing either hepatocyte-specific TBG-Cre recombinase (TBG-Cre) (n=5) or the control vector (TBG-LacZ) (n=5) (*p < 0.05, **p < 0.01; mean \pm S.E.M.). Area under the curve (AUC) for the glucose tolerance test is quantified in the right panel (**p < 0.01; mean \pm S.E.M.). See also Figure S1.

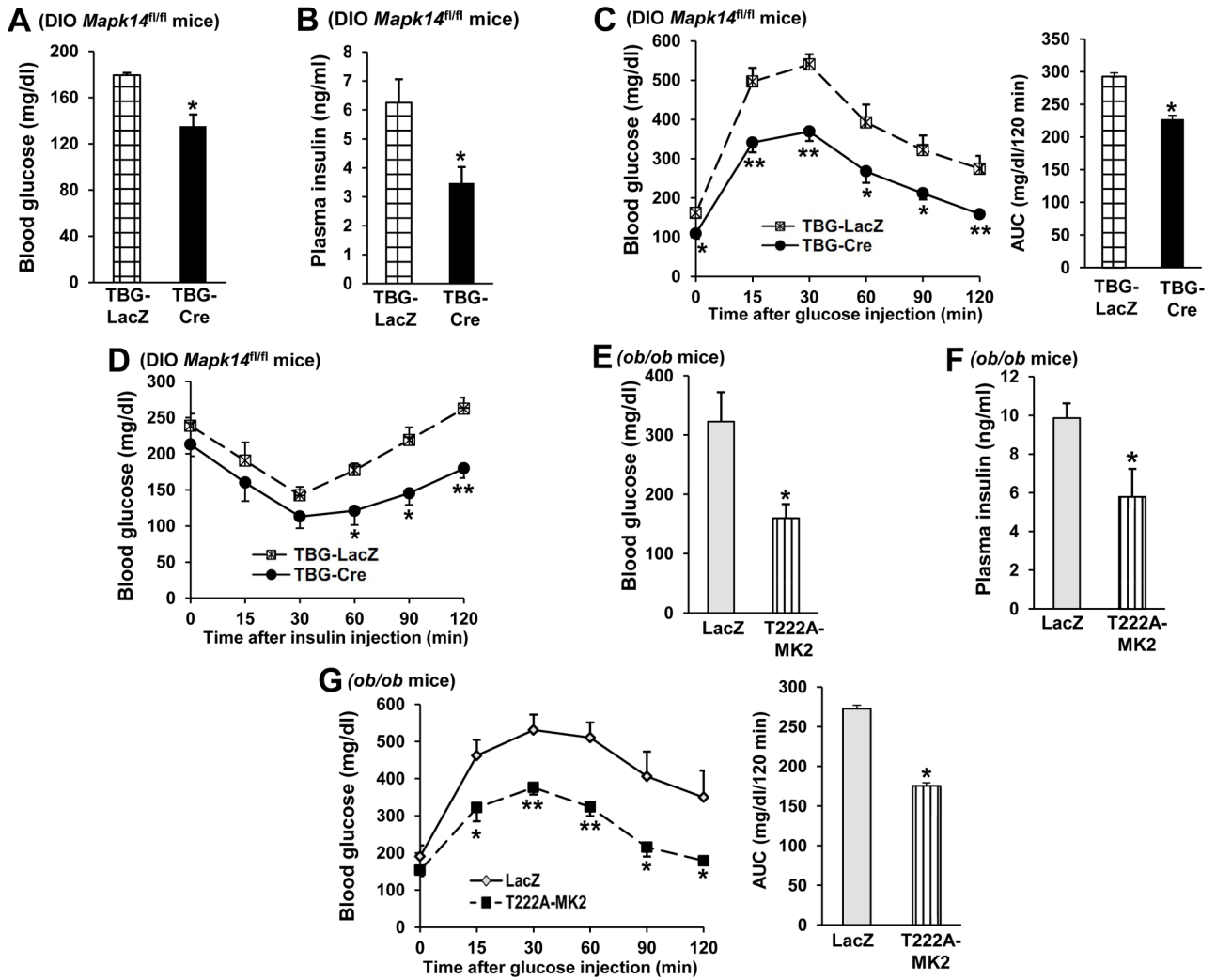


Figure 2. Inhibition or Deletion of p38 α or MAPKAPK2 (MK2) Lowers Plasma Glucose and Insulin and Improves Response to Glucose and Insulin Challenge in Obese mice
 (A–D) Fasting blood glucose, plasma insulin, glucose and insulin tolerance tests in DIO *Mapk14^{fl/fl}* mice after treatment with AAV-TBG-LacZ (n=5) or AAV-TBG-Cre (n=5) (*p <0.05; mean \pm S.E.M.). Area under the curve (AUC) for the glucose tolerance test is quantified in the right panel (*p <0.05; mean \pm S.E.M.). (E–G) Fasting blood glucose and plasma insulin; and blood glucose after glucose challenge in *ob/ob* mice administered 1×10^9 pfu of adeno-LacZ (n=5) or adeno-T222A-MK2 (n=5) (*p <0.05, **p <0.01; mean \pm S.E.M.). Area under the curve (AUC) for the glucose tolerance test is quantified in the right panel (*p <0.05; mean \pm S.E.M.).

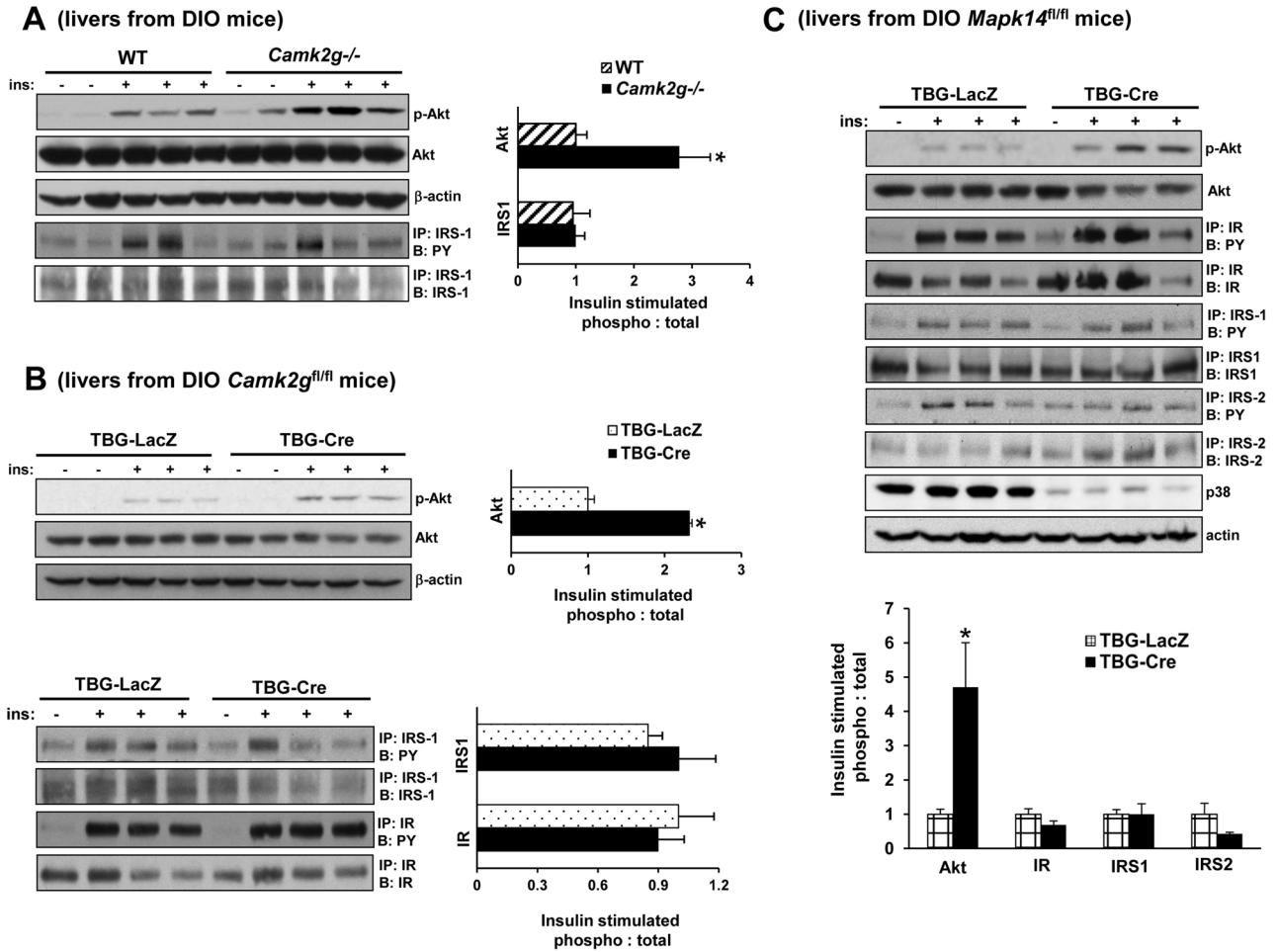


Figure 3. Deletion of CaMKII or p38α Improves Insulin-induced Akt Phosphorylation in Obese Mice

(A) DIO *Camk2g^{-/-}* or WT mice were fasted for 6 h and then injected with 1.5 IU/kg insulin through the portal vein. Total liver extracts were then assayed for p-Akt, total Akt, and β-actin by immunoblot or immunoprecipitated (IP:) for IRS-1 and then assayed by immunoblot (B:) for IRS-1 or for phospho-Tyr (PY). Densitometric quantitation of the immunoblot data is shown in the graph (**p* < 0.05; mean ± S.E.M.). (B) As in (A) except that DIO *Camk2g^{fl/fl}* mice treated with AAV-TBG-LacZ or AAV-TBG-Cre were used and p-IR was also assayed by IP/B (**p* < 0.05; mean ± S.E.M.). (C) As in (B) except that DIO *Mapk14^{fl/fl}* mice were used, and p-IRS-2 was also assayed by IP/B (**p* < 0.05; mean ± S.E.M.). See also Figure S2–3.

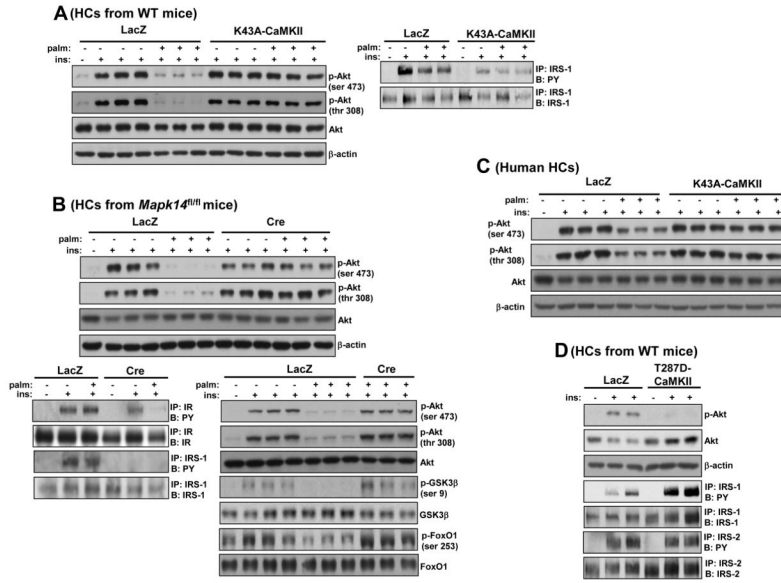


Figure 4. Inhibition of CaMKII or p38 α Improves Insulin-induced Akt Phosphorylation in Palmitate-treated Primary Hepatocytes

(A) Primary HCs from WT mice were transduced with adeno-LacZ or -K43A-CaMKII at an MOI of 10 and then 24 h later incubated with either BSA control or 0.2 mM palmitate for 19 h, with the last 5 h in serum-free media. The cells were then treated with 100 nM insulin or vehicle control for 5 min, and lysates were probed for p-Akt, total Akt, and β -actin by immunoblot (left panel) or immunoprecipitated for IRS-1 and then assayed by immunoblot for the total level of IRS-1 or for phospho-Tyr (PY) (right panel). (B) HCs from *Mapk14^{fl/fl}* mice were transduced with adeno-LacZ or -Cre and 24 h later incubated with palmitate and then insulin as in (A). Lysates were probed for p-Akt, total Akt, β -actin (upper panel), p-GSK3 β , total GSK3 β , p-FoxO1 and total FoxO1 by immunoblot or immunoprecipitated for IR and IRS-1 and then assayed by immunoblot for the total level of the respective proteins or for phospho-Tyr (lower panel). (C) Primary human HCs (metabolism-controlled) were transduced with adeno-LacZ or -K43A-CaMKII at an MOI of 30 and then 36 h later incubated with either BSA control or 0.2 mM palmitate for 10 h, with the last 5 h in serum-free media. The cells were then treated with 100 nM insulin or vehicle control for 5 min, and lysates were probed for p-Akt, total Akt, and β -actin by immunoblot. (D) As in (A) except adeno-T287D-CaMKII was used, and IRS-2 was also assayed. See also Figure S3.

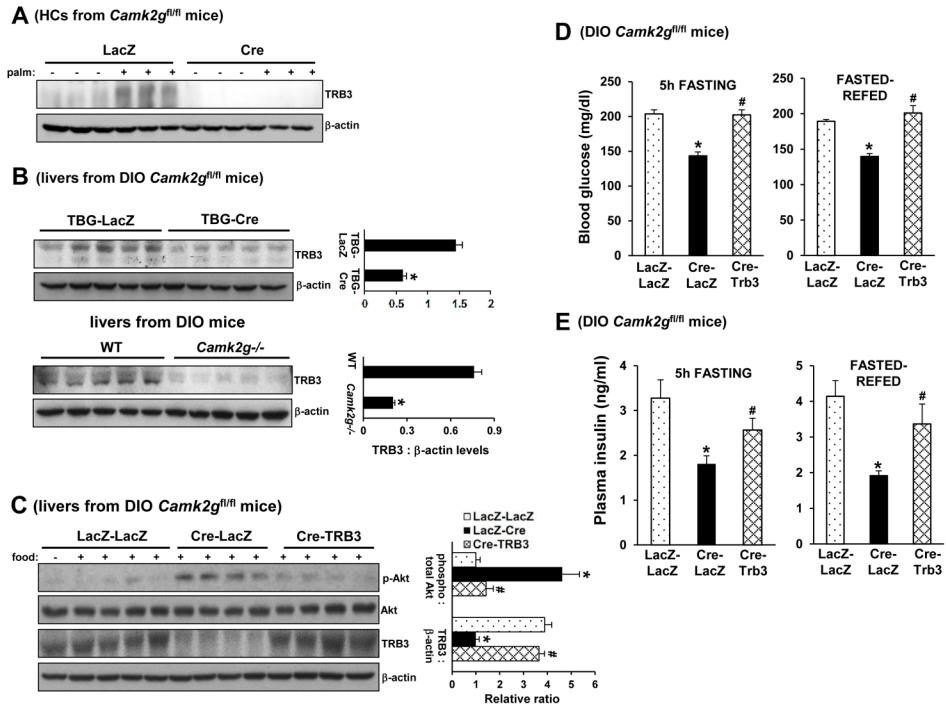


Figure 5. Improvement in Insulin-induced Akt Phosphorylation and Glucose Homeostasis by CaMKII Deficiency are Abrogated by Restoring TRB3
 (A) HCs from *Camk2g^{fl/fl}* mice were transduced with adeno-LacZ or -Cre and then 24 h later incubated with BSA or palmitate (0.2 mM) for 19 h. Lysates were immunoblotted for TRB3 and β -actin. (B) TRB3 and β -actin were probed in livers from DIO WT mice, *Camk2g^{-/-}* mice, or *Camk2g^{fl/fl}* mice treated with TBG-LacZ or TBG-Cre. Densitometric quantification of the immunoblot data is shown in the graph (* $p < 0.05$; mean \pm S.E.M.). (C–E) DIO *Camk2g^{fl/fl}* mice were treated with TBG-Cre or TBG-LacZ, and five days later, half of the TBG-LacZ mice received adeno-TRB3, while the other half received adeno-LacZ control. Livers were assayed for p-Akt, total Akt, TRB3 and β -actin by immunoblotting after fasting the mice for 16 h and then re-feeding them for 4 h. 5 h fasting and fasted-refed blood glucose and plasma insulin were assayed after 4 weeks of treatment (Differing symbols indicate $p < 0.05$; mean \pm S.E.M.). See also Figure S4.

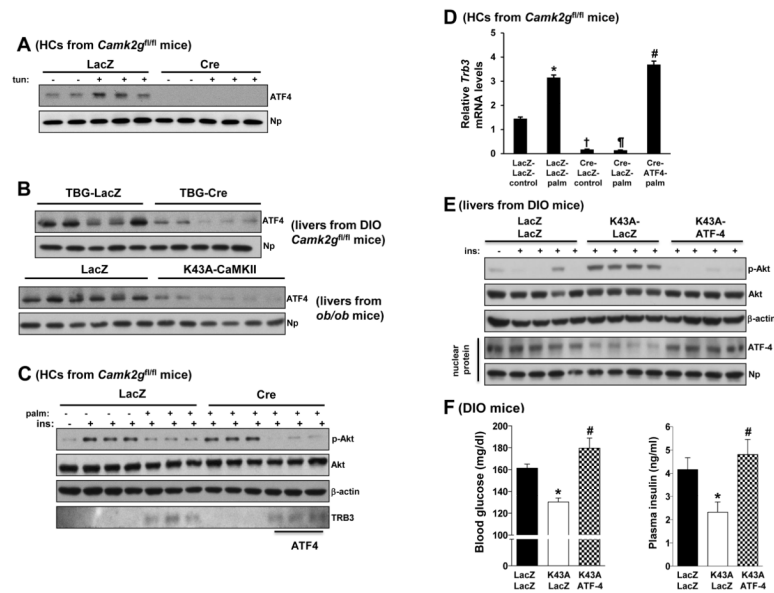


Figure 6. Improvement in Insulin-induced Akt Phosphorylation and Glucose Homeostasis by CaMKII Deficiency are Abrogated by Restoring ATF4
 (A) HCs from *Camk2g^{fl/fl}* mice were transduced with adeno-LacZ or -Cre. 24 h later, cells were incubated with tunicamycin (0.5 μ g/ml) or vehicle control for 4 h. Nuclear lysates were immunoblotted for ATF4 and nucleophosmin (Np) as a loading control. (B) Nuclear ATF4 and nucleophosmin (Np) were probed in livers from DIO *Camk2g^{fl/fl}* mice treated with TBG-Cre or TBG-LacZ or *ob/ob* mice treated with adeno-LacZ or -K43A-CaMKII. (C) HCs from *Camk2g^{fl/fl}* mice were transduced with adeno-LacZ or -Cre and then 4 h later, half of the adeno-Cre transduced cells received adeno-ATF4, while the other half received adeno-LacZ control. After 24 h, the cells were incubated with palmitate and then insulin-induced p-Akt was assayed as in Figure 4. (D) As in (C), except that *Trb3* mRNA was assayed by RT-qPCR (Bars with different symbols are different from each other and control, $p < 0.01$; mean \pm S.E.M.). (E–F) Sixteen-week-old DIO mice were administered adeno-LacZ or -K43A-CaMKII, and then, two days later, half of the adeno-K43A-CaMKII mice received adeno-ATF4 while the other half received adeno-LacZ control. Livers were assayed for p-Akt, total Akt, β -actin and nuclear ATF4 and nucleophosmin (Np) by immunoblotting after insulin injection through portal vein. 5 h fasting blood glucose and plasma insulin were assayed after three weeks of treatment (Differing symbols indicate $p < 0.05$; mean \pm S.E.M.). See also Figure S5.

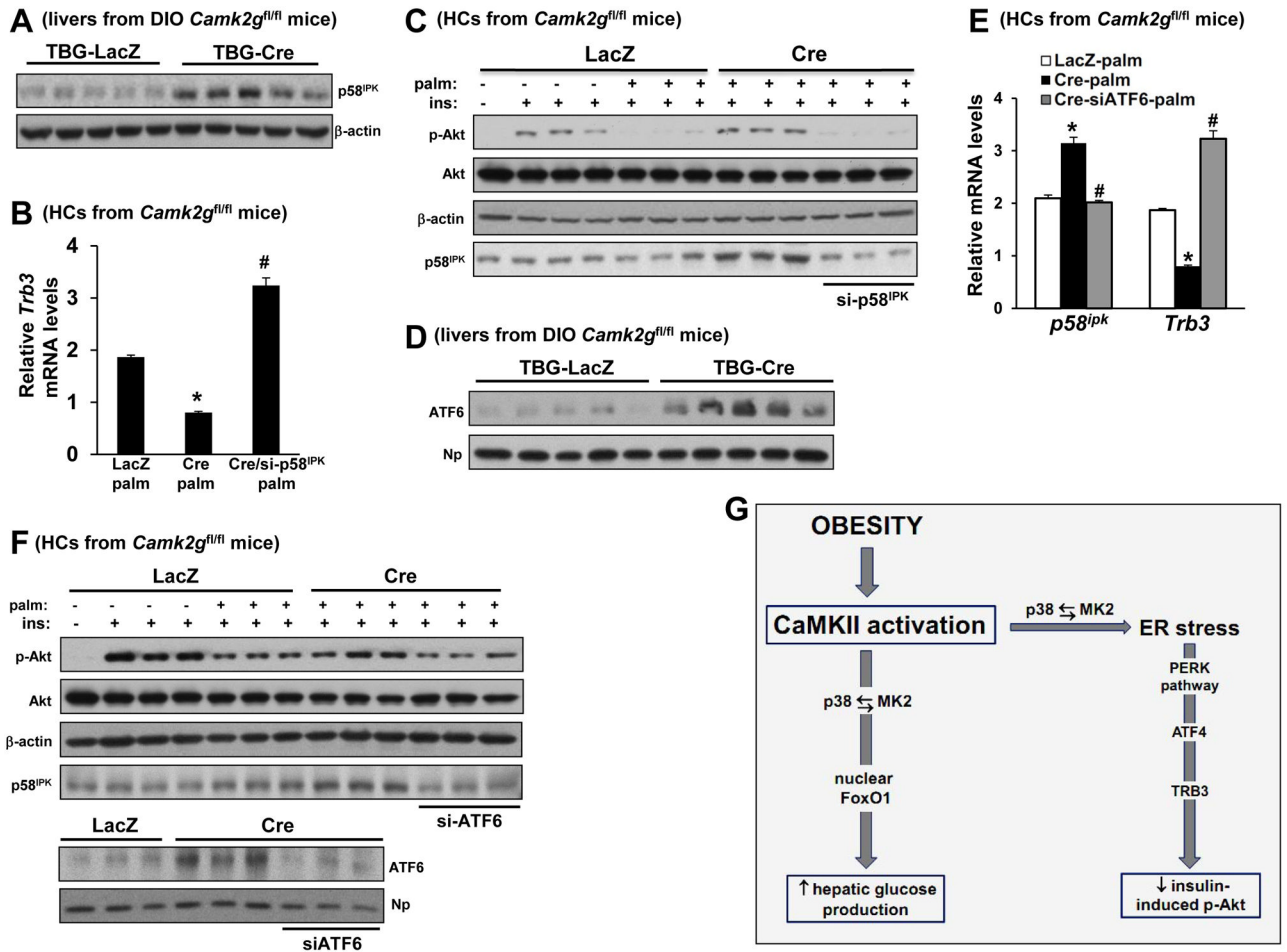


Figure 7. Acute Insulin-induced p-Akt Enhancement in *Camk2g^{-/-}* Hepatocytes is Partially Abrogated by ATF6 Inhibition

(A) p58^{IPK} and β-actin were probed by immunoblot in livers from DIO *Camk2g^{fl/fl}* mice treated with AAV-TBG-Cre or AAV-TBG-LacZ. (B) HCs from *Camk2g^{fl/fl}* mice were pretreated with either scrambled RNA (first 2 bars) or siRNA targeting *p58^{ipk}* (si-p58). After 12 h, the cells were transduced with adeno-LacZ or -Cre. After an additional 24 h, the cells were incubated with BSA control or palmitate (0.2 mM) for 19 h, with the last 5 h in serum-free media. The cells were then assayed for *Trb3* mRNA by RT-qPCR (Bars with different symbols are different from each other and control, $p < 0.05$; mean \pm S.E.M.). (C) As in (B), except the cells were then treated with \pm 100 nM insulin for 5 min, and lysates were immunoblotted for p-Akt, total Akt, β-actin, and p58^{IPK} by immunoblot. (D) Nuclear ATF6 and nucleophosmin (Np) were probed by immunoblot in livers from DIO *Camk2g^{fl/fl}* mice treated with AAV-TBG-Cre or AAV-TBG-LacZ. (E) As in (B), except siRNA targeting *Atf6* (siATF6) was used, and *p58^{ipk}* mRNA was also assayed; first 2 bars in each group received scrambled RNA (Bars with different symbols are different from each other and control, $p < 0.05$; mean \pm S.E.M.). (F) HCs were prepared as in (C) except siRNA targeting *Atf6* (siATF6) was used. Lysates were immunoblotted for p-Akt, total Akt, β-actin and p58^{IPK} by immunoblot. In the lower blot, nuclei from a parallel set of cells treated with palmitate were probed for ATF6 and nucleophosmin (Np) by immunoblot. (G) The data here and previously (Ozcan et al., 2012) support an integrated scheme in which CaMKII mediates two key pathways in the setting of obesity, one contributing to defective insulin signaling and the

other to excessive HGP. Thus, inhibition of liver CaMKII or its downstream agent p38 improves the two cardinal features of T2D. See also Figure S6.